



Contents lists available at SCCE

Journal of Soft Computing in Civil Engineering

Journal homepage: www.jsoftcivil.com



Experimental Investigation and Modeling of Aeration Efficiency at Labyrinth Weirs

A. Singh¹, B. Singh^{2*} , P. Sihag³

1. Civil Engineering Department, National Institute of Technology, Kurukshetra, India

2. Civil Engineering Department, Panipat Institute of Engineering and Technology, Samalkha, India

3. Civil Engineering Department, Shoolini University, Solan, India

Corresponding author: balrajzinder@gmail.com

 <https://doi.org/10.22115/SCCE.2021.284637.1311>

ARTICLE INFO

Article history:

Received: 04 May 2021

Revised: 26 June 2021

Accepted: 09 August 2021

Keywords:

Labyrinth weir;

Aeration efficiency;

SVM;

RF;

M5P.

ABSTRACT

For maintaining healthy streams and rivers, a high concentration of oxygen is desired and hydraulic structures act as natural aerators where oxygen transfer occurs by creating turbulence in the water. Aeration studies of conventional weirs are carried out widely in the past but at the same time, labyrinth weirs, where the weir crest is cranked thereby enhancing their crest length, have got a little notice. The test records were obtained through 180 laboratory observations on nine physical models to estimate aeration efficiency (E_{20}) at labyrinth weirs (LWs). The E_{20} increases with the number of key as well as drop height and it is found to be highest for rectangular shape in comparison of the triangular and trapezoidal LWs, however, E_{20} decreases with the increase of discharge. Further, this work unravels the novel idea and potential of the M5P model tree (M5P), support vector regression machine (SVM), and Random Forest (RF) methods for estimation of aeration efficiency (E_{20}) at LWs. The results depicted that the RF model performs best in determining the E_{20} at LWs. The results of sensitivity analysis further illustrated that drop height is the parameter that affects the prediction of E_{20} at the LWs most.

How to cite this article: Singh A, Singh B, Sihag P. Experimental Investigation and Modeling of Aeration Efficiency at Labyrinth Weirs. J Soft Comput Civ Eng 2021;5(3):15–31. <https://doi.org/10.22115/scce.2021.284637.1311>.

2588-2872/ © 2021 The Authors. Published by Pouyan Press.

This is an open access article under the CC BY license (<http://creativecommons.org/licenses/by/4.0/>).



1. Introduction

Maintenance of a high concentration dissolved oxygen (DO) of natural water bodies is important and this can be achieved by generating eddies and turbulence in the water. One technique of producing such eddies is allowing flow over hydraulic structures. In an irrigation and drainage system, oxygen transfer occurs on the surface of the flow as flowing water moves down through the waterway, and to manage that agricultural water, hydraulic structures like weirs are preferably used, which indirectly improve this oxygen aeration hugely.

Weirs are a basic hydraulic structure that is employed either for flow measurement or to retain water or to maintain water level or for flow diversion. In contrast to the classical weirs, nonlinear weirs can enhance the capacity of the flow for the same cross-sectional width without increasing the overflow depth. Classical and labyrinth weirs differ in geometry and the layout of their walls. Gentilini [1] was the first researcher who investigated the performance of LWs but the modern labyrinth weirs were designed by Taylor [2] and improved by Hay and Taylor [3], however, comparative performance of an inverted and normal LW was carried out by Crookston and Tullis [4]. The flow characteristics of arched LWs were studied by Christensen (2012) and Tullis [5] studied geometric changes and their impact on labyrinth efficiency and predictions of the design method.

The aeration basis of the classical weirs was first investigated by Gameson [6], then a plethora of authors assessed the aeration performance of these normal weirs [7–11]. However, very few works have been reported on non-linear weirs include Wormleaton & Soufiani [12] and Wormleaton & Tsang [13] who have shown that triangular and rectangular planform LWs respectively do have better oxygen aeration performance over conventional linear weirs and the reason attributed is two folds; one is the geometry of the nonlinear weirs which affords an additional sill (crest) length and second is collision and interference of overfall jets, both of which upturn the turbulence and air entrapment in plunging waterjet and make them extra efficient natural aerators.

Alternatively, AI-based data-driven techniques (SVM, M5P, RF, etc.) can be invoked for modeling the oxygen transfer at Labyrinth weirs. Nowadays, AI-based techniques, due to their simplicity, in-built intelligence, and reliability, have been gradually used in the modeling process of complex problems of hydraulic structure and environment engineering [14–27].

To sum up, many works are present in the literature that deals with aeration characteristics of conventional weirs and the hydraulic aspect of the labyrinth weirs in general but still works reported on aeration characteristics of the labyrinth weirs are very few, and modeling related work is missing. Thus, the present work is arranged into two sections. The initial section describes the experimental study of the oxygen transfer at different geometry, a different number of keys (different cycle), and drop height of LWs while the second section deals with modeling techniques; SVM, M5P, and RF utilized in the estimation of aeration efficiency (E_{20}). In addition, a comparison of the current study is also made out with previous studies available in the text.

2. Methods

2.1. Oxygen transfer mechanism at drop structures

The oxygen transfer mechanism, itself is a very complex process and different types. The mechanism principle in the drop structures like cascades or step channels is entirely different from that of drop structures like weirs. In cascades, the overflow can be broadly divided into skimming flow and nappe flow as shown in Figure-1. For the skimming flow, overflow discharge is high or cascade step is narrow while jet flow occurs either overflow discharge is low or cascade step is wide. Further, the water skims over the faces and corners of step in skimming flow (Figure-1i) and is retarded due to the development of the circulating region which further enhances the self-aeration process by momentum exchange in the flow while in the case of jet flow, aeration takes place with the steps which act as a series of overfalls where the water is free-falling from one step to other as shown in Figure-1ii [28]. However, in the case of drop structure as a weir, oxygen transfer depends upon the plunging velocity, roughness, shape, and geometry of the receiving water aeration pool. Both the shape and depth of the water aeration pool control the residence time and penetration depth of the air bubbles. A self-explanatory sketch showing the mechanisms of oxygen transfer different at different stages (type-a, b, c & d) through a free-falling jet over the weir [29] and is depicted in Figure 2.

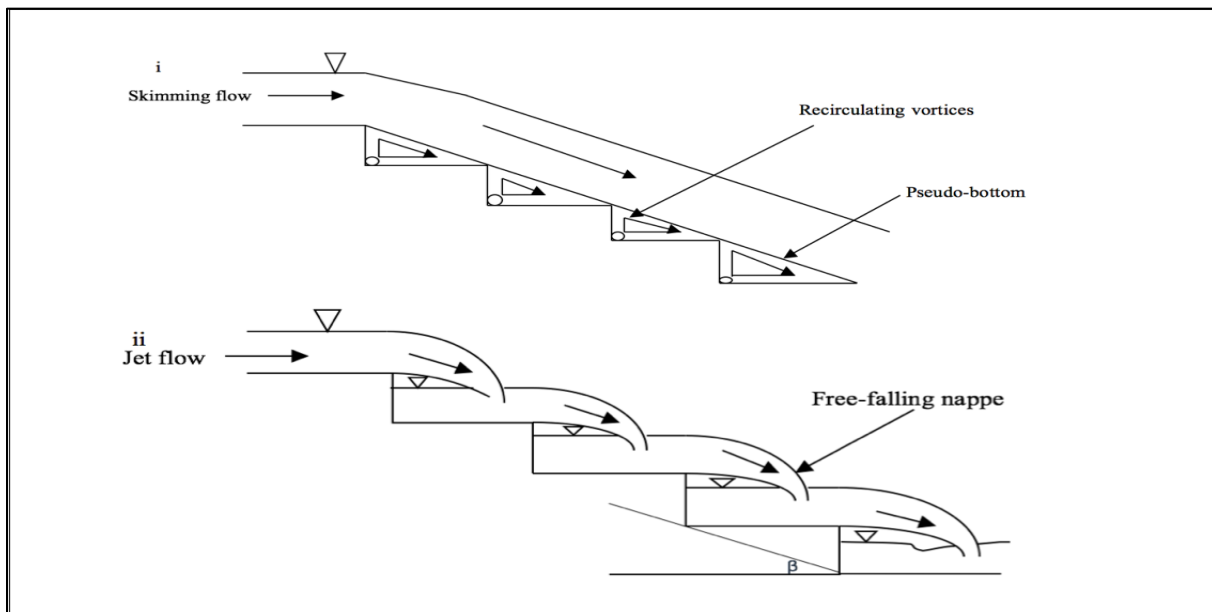


Fig. 1. Oxygen transfer mechanism over cascades: (i) Skimming flow and (ii) Jet flow (after Ohtsu et al., 2001).

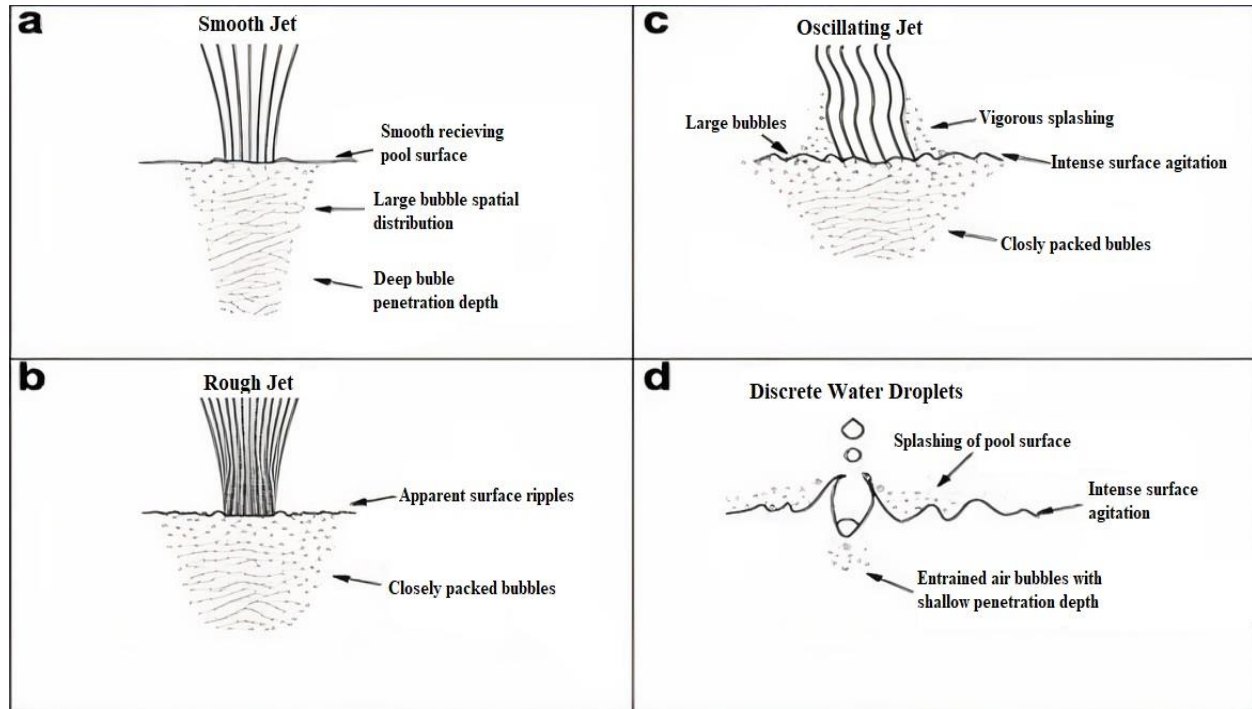


Fig. 2. Oxygen transfers mechanism at different stages (type-a, b, c & d) in overflow plunging water from the weir (after Tsang 1987).

2.2. Oxygen aeration parameters and previously developed popular classical models

The oxygen aeration efficiency, E , at any temperature, $T^{\circ}\text{C}$ is outlined as (Gulliver et al., [30])

$$E = 1 - \frac{1}{r} = \frac{\frac{C_D}{S} - \frac{C_U}{S}}{C_S - \frac{C_U}{S}} \quad (1)$$

Where $\frac{C_D}{S}$ and $\frac{C_U}{S}$ are subscripts showing downstream and upstream locations respectively and 's' subscript shows saturation while C stands for the DO concentration (ML^3) in ppm while r denotes the oxygen deficit ratio. Further, E is aeration efficiency (oxygen transfer) at any temperature, $T^{\circ}\text{C}$. The general aeration efficiency, E , is normalized to 20°C and denoted as E_{20} for this study and is given by

$$1 - E_{20} = 1 - \frac{1}{E^{(1.0+0.02108(T-20)+8.261 \times 10^{-5}(T-20)^2)}} \quad (2)$$

There are many factors on which E_{20} of labyrinth weirs is dependent on the aeration process. Only a few works on the estimation of E_{20} of labyrinth weir are present in the literature which only follows the classical regression methods. The classical methods are either underestimated or over-estimated the labyrinth weir E_{20} . Hence, in this investigation, above-mentioned methods are assessed and checked the performance by test dataset and the performance is assessed using these experimental calculated datasets.

Avery and Novak [9] examined the oxygen transfer performance for 4 classical weirs and obtained the subsequent model in terms of Froude numbers (F_r), and Reynolds number (R_e).

$$E_{15} = 1 - [1 + 0.627 \times 10^{-4} F_r^{1.78} R_e^{0.53}]^{-1} \quad (3)$$

In which, F_r = Froude number, R_e = Reynold number and q_j = discharge, and D = drop height.

But, Avery and Novak's model needs to be normalized to 20⁰C. This was made using the formula of Tebbutt et al. [31], given as

$$\frac{E_T(1-E_{20})}{E_{20}(1-E_T)} = [1 + 0.0355(T - 20)] \quad (4)$$

where E_T = aeration efficiency at any temperature T⁰C.

Tsang [29] modified the above Avery and Novak's model and developed his classical model for aeration study of labyrinth weirs which is given as

$$E_{20} = 1 - [1 + 0.762 \times 10^{-4} F_r^{1.78} R_e^{0.53}]^{-1} \quad (5)$$

Wormleaton and Tsang [13] conducted many tests in the laboratory on rectangular-shaped LWS for assessment of aeration efficiency and given the following model

$$E_{20} = 1 - [1 + 0.385 \times 10^{-6} F_r^{2.297} R_e^{0.684}]^{-1} \quad (6)$$

2.3. Experimentation setup and investigation

Oxygen transfer tests were performed using a tilting flume in a laboratory of NIT, Kurukshetra (India). The test flume utilized in this investigation, has a length of 4 m, a width of 0.25 m, and a depth of 0.50 m with a range of water discharge of around 1-5L/s. The schematic of the experimental test was shown in Figure-3. The test models were fabricated using a 5 mm thick good quality waterproof plywood sheet. This PKW - models were mounted across the full width of the flume at its tail end and were sealed with waterproof materials to ensure no leakage, for all runs clean drinking water was used. It was ensured that the depth of water in the aeration tank was maintained throughout greater than penetration depth for every test [9]. The jet of water over the test labyrinth weir was allowed to be plunged into the downstream aeration cum supply tank, whose height could be adjusted using the lifting jacks provided at both upstream and downstream of the flume. Flume was provided with the re-circulating closed device which was employed for continuously feeding the flume by redrawing water from the tank with a dimension of 125 cm length, 60 cm width, and 60 cm depth using a 5 mm thick good quality painted plywood sheet.

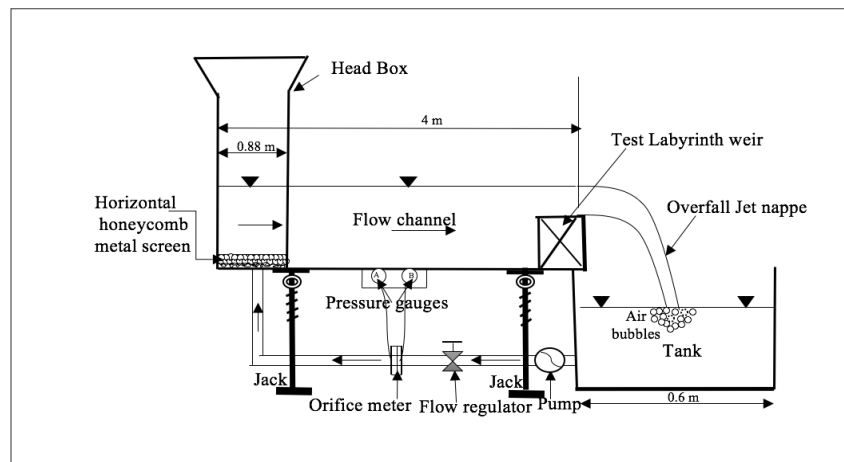
The test model featured nine exchangeable labyrinth weirs: 3-rectangular weir; 3-triangular weirs and 3-trapezoidal weirs having common width (W) and height (P) of 26.3 cm and 12.5 cm respectively. Different models have been created utilizing the number of keys, drop height, and shape of labyrinth weirs as revealed in Table 1.

Table 1

Summary of the test models for variation discharge from 1-5 l/s.

| Sr. No | Model | Number of Key | Drop Height (m) | Shape | Sr No | Model | Number of Key | Drop Height(m) | Shape |
|--------|-------|---------------|-----------------|------------|-------|-------|---------------|----------------|-------------|
| 1 | M1 | 1 | 0.80 | Triangular | 19 | M19 | 1 | 0.9 | Rectangular |
| 2 | M2 | 2 | 0.8 | Triangular | 20 | M20 | 2 | 0.9 | Rectangular |
| 3 | M3 | 3 | 0.8 | Triangular | 21 | M21 | 3 | 0.9 | Rectangular |
| 4 | M4 | 1 | 0.85 | Triangular | 22 | M22 | 1 | 0.95 | Rectangular |
| 5 | M5 | 2 | 0.85 | Triangular | 23 | M23 | 2 | 0.95 | Rectangular |
| 6 | M6 | 3 | 0.85 | Triangular | 24 | M24 | 3 | 0.95 | Rectangular |
| 7 | M7 | 1 | 0.9 | Triangular | 25 | M25 | 1 | 0.8 | Trapezoidal |
| 8 | M8 | 2 | 0.9 | Triangular | 26 | M26 | 2 | 0.8 | Trapezoidal |
| 9 | M9 | 3 | 0.9 | Triangular | 27 | M27 | 3 | 0.8 | Trapezoidal |
| 10 | M10 | 1 | 0.95 | Triangular | 28 | M28 | 1 | 0.85 | Trapezoidal |
| 11 | M11 | 2 | 0.95 | Triangular | 29 | M29 | 2 | 0.85 | Trapezoidal |
| 12 | M12 | 3 | 0.95 | Triangular | 30 | M30 | 3 | 0.85 | Trapezoidal |
| 13 | M13 | 1 | 0.8 | Triangular | 31 | M31 | 1 | 0.9 | Trapezoidal |
| 14 | M14 | 2 | 0.8 | Triangular | 32 | M32 | 2 | 0.9 | Trapezoidal |
| 15 | M15 | 3 | 0.8 | Triangular | 33 | M33 | 3 | 0.9 | Trapezoidal |
| 16 | M16 | 1 | 0.85 | Triangular | 34 | M34 | 1 | 0.95 | Trapezoidal |
| 17 | M17 | 2 | 0.85 | Triangular | 35 | M35 | 2 | 0.95 | Trapezoidal |
| 18 | M18 | 3 | 0.85 | Triangular | 36 | M36 | 3 | 0.95 | Trapezoidal |

The azide modification technique was employed for measurement of the dissolved oxygen and each run was resumed by filling the tank with a known volume of clean drinking water. An appropriate amount of sodium sulfite (Na_2SO_3) and cobalt chloride (CoCl_2) which itself acts as catalyst were added to bring DO concentration of water in the tank between 1 and 2 ppm [18]. First of all, before the start of the run, a water sample from the tank was collected for measurement of initial DO ($C_{d/s}$). Thereafter, the flume was allowed to run for a certain period so that the DO concentration of water in the tank does not reach the saturation value (C_s) at any tested temperature ($T^\circ\text{C}$) and the final value of DO ($C_{d/s}$) was computed. The water temperature in the tank was computed by a thermometer with the least accuracy of $\pm 0.1^\circ\text{C}$. The same steps were continued for various runs employing nine different labyrinth weirs having different geometry and number of keys as mentioned in Table 1 and the value of E_{20} was then computed by using equations-1 & 2.

**Fig. 3.** Schematic view of experimentation.

A graph between E_{20} at LWs and discharge for a different model (Table 1) have been shown in Figure 4. From the perusal of this figure, it is evident that with the increase in discharge(q), E_{20} decreases, by and large for every model and the reason may be attributed that water possesses a smaller surface area and smaller time to be in contact with the atmosphere as discharge thereby velocity increases. Further, the E_{20} is greatest with the rectangular labyrinth weir and lowest with the triangular weir for either single or multiple-key rectangular LWs. Among the different geometries (triangular rectangular and trapezoidal) and the number of keys (1, 2 & 3) used in the study, the highest value 3- key labyrinth weir in every shape was found to be more efficient in terms of E_{20} .

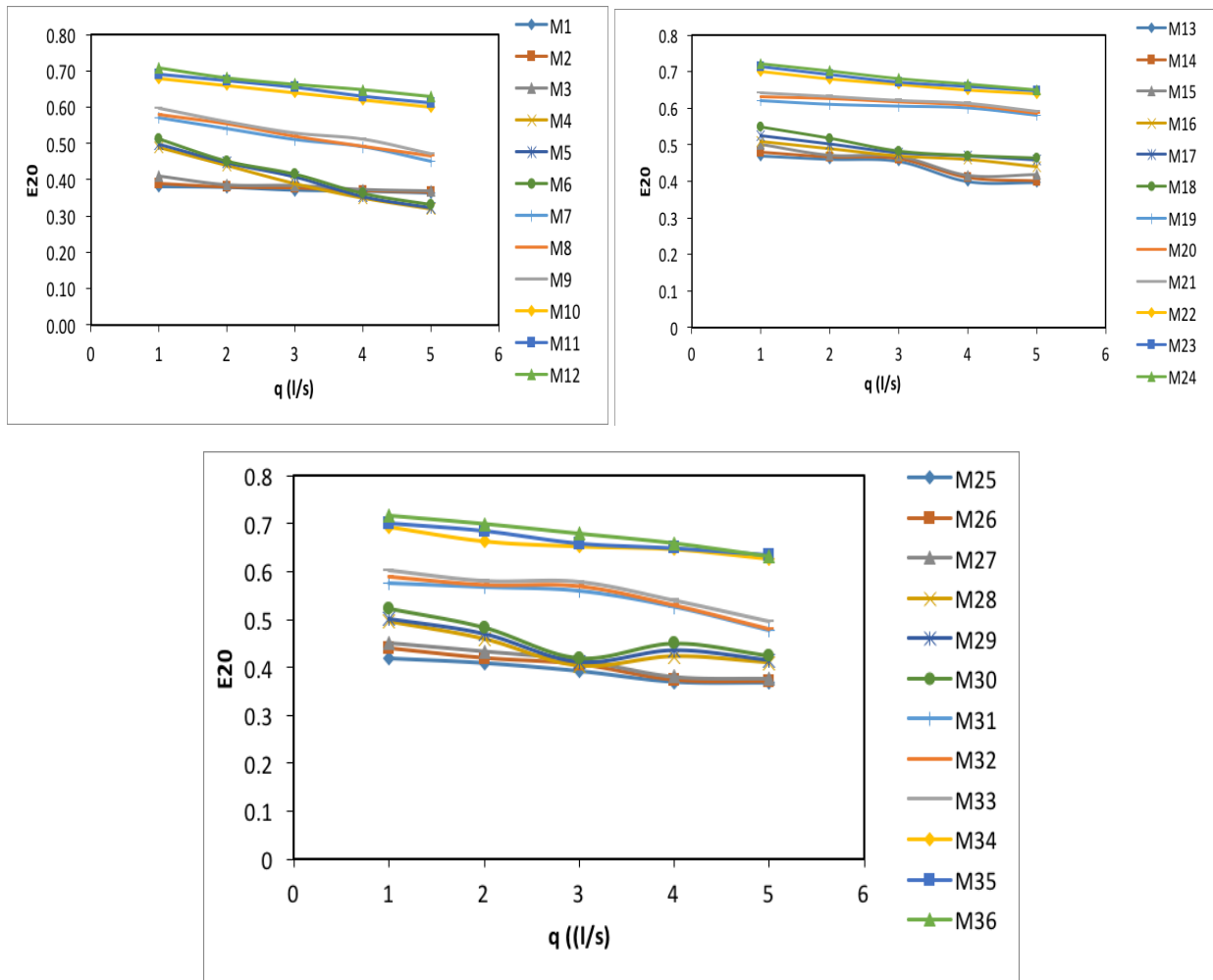


Fig. 4. Variation of E_{20} with discharge for various models.

2.4. Dataset

To evaluate the efficacy of SVM, RF, and M5P soft computing models to predict the aeration efficiency at LWs. The investigation contains a total of 180 experimental observations. Out of these, 126 readings were selected for training purposes, whereas the rest 54 were selected for testing purposes. To estimate the aeration efficiency at weirs, seven input parameter Froude number (Fr), Reynolds number (Re), Numbers of keys (N), the ratio of head and width of the

channel (H/W), the ratio of drop height and width of the channel (D/W), the ratio of crest length and width of the channel (L/W), and Shape Factor (SF) were used whereas aeration efficiency (E_{20}) was output. The shape factor has been assumed as 1 for triangular, 1.5 for trapezoidal and 2 for rectangular weirs. Table 2 provides the descriptive summary of training as well as the testing dataset.

Table 2
Descriptive summary.

| Parameters | Training | | | | | |
|------------|----------|-------|---------|---------|-------|-------|
| | Min. | Max. | Mean | S. Dev. | Kur | Ske |
| Fr | 8.90 | 22.64 | 13.63 | 4.22 | -0.42 | 0.91 |
| Re | 2000 | 10000 | 6079.37 | 2855.46 | -1.32 | -0.02 |
| N | 1 | 3 | 2.02 | 0.81 | -1.47 | -0.03 |
| H/W | 0.168 | 0.76 | 0.50 | 0.20 | -0.85 | -0.51 |
| L/W | 1.32 | 3.94 | 2.54 | 0.79 | -0.82 | 0.30 |
| D/W | 3.2 | 3.8 | 3.49 | 0.22 | -1.33 | 0.03 |
| SF | 1 | 2 | 1.49 | 0.41 | -1.51 | 0.03 |
| E_{20} | 0.32 | 0.723 | 0.52 | 0.11 | -1.23 | 0.15 |
| | Testing | | | | | |
| Fr | 8.90 | 22.64 | 14.05 | 4.40 | -0.67 | 0.84 |
| Re | 2000 | 10000 | 5814.81 | 2808.84 | -1.26 | 0.04 |
| N | 1 | 3 | 1.96 | 0.85 | -1.61 | 0.07 |
| H/W | 0.168 | 0.76 | 0.49 | 0.20 | -0.96 | -0.48 |
| L/W | 1.32 | 3.94 | 2.52 | 0.76 | -0.73 | 0.35 |
| D/W | 3.2 | 3.8 | 3.51 | 0.23 | -1.45 | -0.07 |
| SF | 1 | 2 | 1.52 | 0.41 | -1.52 | -0.07 |
| E_{20} | 0.362 | 0.714 | 0.53 | 0.11 | -1.42 | 0.09 |

Where min. = minimum, max. = maximum, s. dev. = standard deviation, ske = skewness and kur = kurtosis

2.5. Artificial Intelligence-based techniques

2.5.1. Support vector machine (SVM)

The concept of SVM was proposed by Vapnik in 1995. It is based on the structural risk minimization principle from statistical learning theory. SVM has increased attractiveness due to solving and explaining nonlinear complex input-output relationship-based numerical problems. SVM has been successfully used in classification and regression by several researchers in various research fields such as civil, hydraulics, water resources, electrical, mechanical engineering, financial, medical, biomedical, chemistry, and others [32]. Details of SVM theory

have been presented in several articles and reports [27,33] only a concise preface is listed here. The least-squares method (Cristianini et al. 1999) recommends selecting the variables to optimize the sum of the squared deviations of the data $\sum_{i=f_1}^l (y_i - \langle w \cdot x \rangle - b)^2$. To permit for selected deviation among the final outputs y_i and the function $f(x) = \langle w \cdot x \rangle + b$, the following boundary conditions are invoked: $y_i - w \cdot x - b < \varepsilon$ & $y_i - w \cdot x + b \leq \varepsilon$. This can be seen as a band or a tube around the hypothesis function $f(x)$ with points beyond the tube considered as calibrating errors, otherwise called slack variables (readers refer to Vapnik [32] for more information).

2.5.2. M5P model tree

M5P model tree was first time presented by Quinlan [34]. It is an effective and correct method for developing the relationships amongst various variables for complex problems and huge information. There is a chance of over-fitting in the development of the model tree (MT). The correctness of the model surges monotonically as the tree develops. A technique for decreasing the over-fitting is named 'pruning'. In the last stage, sharp discontinuities that take place among nearby models at nodes of the pruned tree were adjusted by the smoothing process. In nutshell, the three main stages for M5P model tree growth are development, pruning; and smoothing. M5P model tree development tries to maximize the reduction in expected error which is known as the standard deviation reduction (SDR). SDR is computed as

$$SDR = sd(F) - \sum \frac{|F_i|}{|F|} sd(F_i) \quad (7)$$

Where A signifies a set of cases; A_j represents the j^{th} subset of cases that the outcome from the tree splitting based on attributes and sd is the standard deviation.

2.5.3. Random Forest (RF)

RF is first time presented by Breiman [35]. It is applied to develop a model which contains a collection of numerous trees. Each tree symbolizes the specific classification and selects the classification accordingly. The RF technique chooses the classification that has the higher option in the forest. The tree is complete if N is the number of instances in the training set. N events arbitrarily by substitution from the original dataset may be the input dataset to mature and complete the tree. The design of RF regression permits a tree to develop to acquire the highest and mature height of a new training dataset utilizing the blending of parameters. The m parameters are chosen arbitrarily from K input parameters for the best split and the value of m ought to be less than K and fixed. The tree is fully grown without cutting to a fair degree. RF can efficiently and correctly be used with huge and intricate data comprising numerous input parameters.

2.6. Selection of the best fitting model

To assess the capability of studied models, two statistic values were calculated using the following equations [36]. Models with the most excellent goodness-of-fit were chosen as the best models.

Coefficient of correlation (CC):

$$CC = \frac{N \sum XY - (\sum X)(\sum Y)}{\sqrt{N(\sum X^2) - (\sum X)^2} \sqrt{N(\sum Y^2) - (\sum Y)^2}} \quad (8)$$

Root mean square error (RMSE)

$$RMSE = \sqrt{\frac{1}{N} (\sum_{i=1}^N (X - Y)^2)} \quad (9)$$

where X, Y, and N are observed E_{20} , predicted E_{20} , and a number of data, respectively.

3. Results

To assess the accuracy of SVM, M5P, and RF-based models in predicting the aeration efficiency at Labyrinth weir. Experimental data was used in the current study for model development and validation. The data set was divided into two groups. The larger group is used for model development and the smaller group is used to test the models. CC and RMSE were used to check the accuracy of developed models. Many manual trials were done to find the optimum values of user-defined parameters for the best models. The detail of user-defined parameters is listed in Table 3.

Table 3

Primary parameters.

| AI-based data driven techniques | Primary parameters | |
|---------------------------------|--------------------|---------------------------------|
| SVM | PUK | $C = 2, \omega = 1, \sigma = 1$ |
| | RBF | $C = 2, \gamma = 2$ |
| RF | $k=10, m=1, I=100$ | |
| M5P | $m=4$ | |

Figure 5 shows a plot among observed and predicted aeration efficiency at Labyrinth weir using Pearson VII and radial basis kernel function-based SVM models. To Study, the Scatter plot indicates that values predicted using SVM_PUK and SVM_RBF are close to the line of perfect agreement. Table 4 shows that SVM_PUK works better than the SVM_RBF model. SVM_PUK and SVM_RBF-based models were suitable for the prediction of aeration efficiency at the Labyrinth weir.

Figure 6 shows a plot among observed and predicted aeration efficiency at Labyrinth weir using RF and M5P models. To Study, the Scatter plot indicates that values predicted using RF and M5P are close to the line of perfect agreement. Table 4 shows that RF works better than the M5P model. RF and M5P based models were suitable for the prediction of aeration efficiency at the Labyrinth weir.

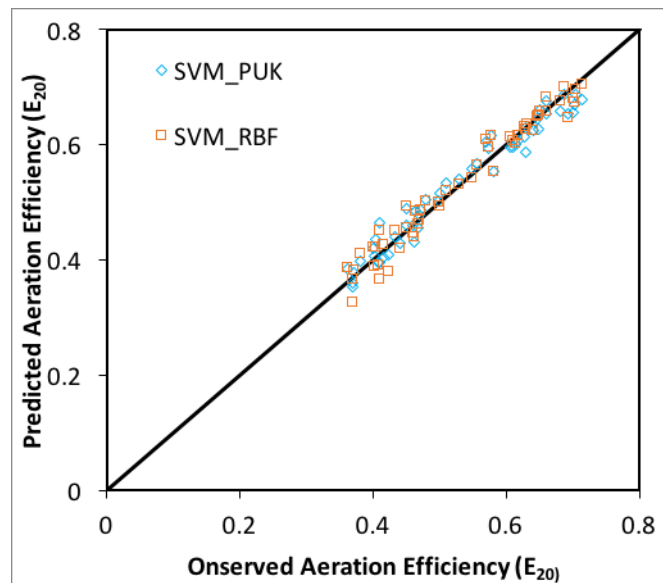


Fig. 5. Scatter Plot of SVM models for testing dataset.

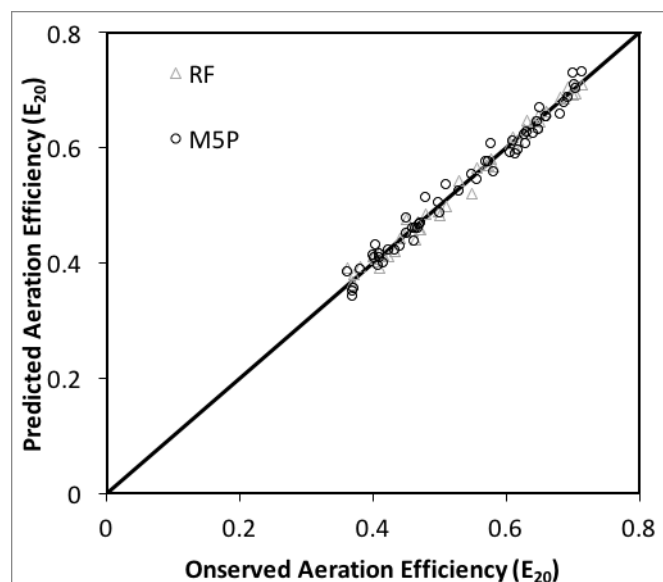


Fig. 6. Scatter Plot of RF and M5P models for testing dataset.

Table 4

Performance of AI-based data-driven techniques.

| Approaches | | SVM_PUK | SVM_RBF | RF | M5P | Avery and Novak [9] | Tsang [29] | Wormleaton and Tsang [13] |
|------------------|------|---------|---------|--------|--------|---------------------|------------|---------------------------|
| Training dataset | CC | 1 | 0.9988 | 0.9988 | 0.9909 | 0.5767 | 0.5783 | 0.8411 |
| | RMSE | 0.0007 | 0.0055 | 0.0056 | 0.0149 | 0.1761 | 0.1387 | 0.0985 |
| Testing dataset | CC | 0.9815 | 0.9813 | 0.9948 | 0.9898 | 0.5839 | 0.5856 | 0.8476 |
| | RMSE | 0.0218 | 0.0213 | 0.0112 | 0.0158 | 0.1844 | 0.1459 | 0.1031 |

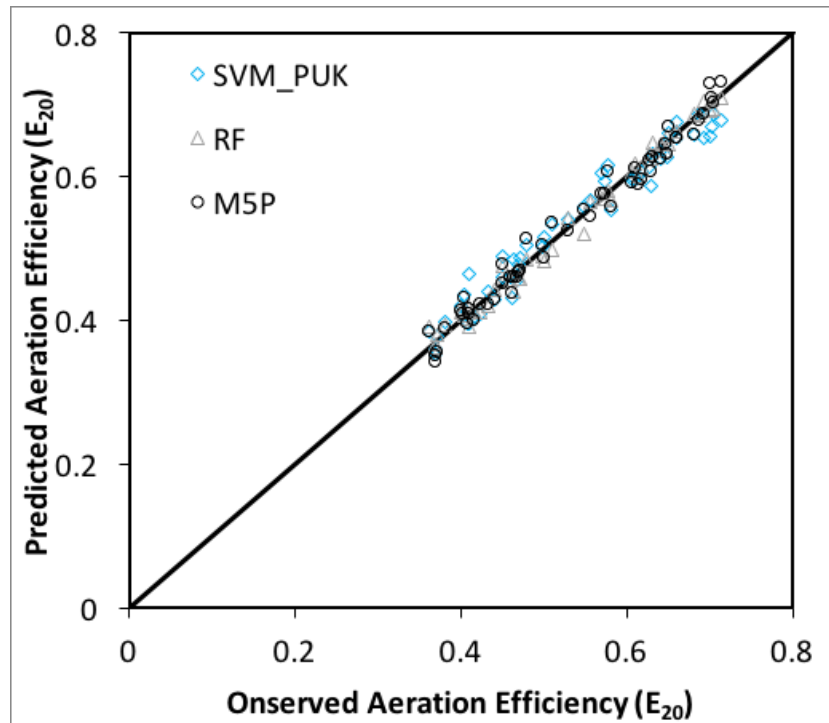
**Fig. 7.** Scatter Plot of SVM, RF, M5P models for testing dataset.

Figure 7 shows a plot among observed and predicted aeration efficiency at Labyrinth weir using SVM, RF, and M5P models. Predicted values using the RF-based model are very closer to the line of perfect agreement. Table 4 shows that RF works better than SVM, M5P model. RF model is more suitable than other discussed models for the prediction of aeration efficiency at Labyrinth weir.

4. Discussion

This investigation aimed to study and model the aeration efficiency at Labyrinth weirs using SVM, RF, and M5P modeling techniques. Total 18 models (M1-M18) were created using the

different values of the number of keys, drop height, and shape of labyrinth weirs. The values of CC and RMSE for the vest model; RF, were 0.9948 and 0.0112 respectively, for the testing phase. The scatters of RF also lie on the agreement line (shown in Figure 7). Furthermore, a comparison was done with the conventional models; Avery and Novak [9], Tsang [29], and Wormleaton and Tsang [13]. Apart from the Wormleaton and Tsang [13] equation, another conventional equation has very high errors when estimating the Aeration Efficiency (E_{20}) at Labyrinth weir on this dataset. Results of every conventional equation were plotted versus the observed Aeration Efficiency (E_{20}) and are shown in Figure 8. Standard error indices containing CC and RMSE were selected to measure the exactness of conventional equations. As shown in Table 4 and Figure 8, the Wormleaton and Tsang [13] equation with CC = 0.8476 and RMSE = 0.1031 is the most precise one amid the conventional equation.

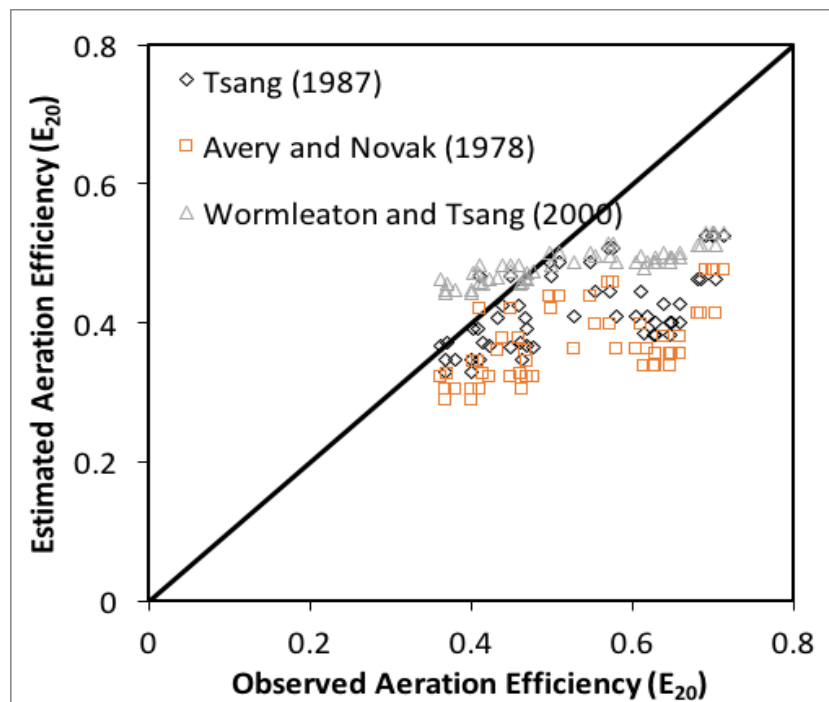


Fig. 8. Scatter Plot of conventional models for testing dataset.

The performance of artificial intelligence techniques and conventional equations are presented in Figure 9 and Table 4. Figure 9 and Table 4 suggest that the performance of the soft computing-based model is better than conventional equations. RF model outperforms conventional equations and soft computing-based models with CC= 0.9948 and RMSE =0.0112 for the testing stage. Hence, with the help of the RF technique, the aeration efficiency can be determined at any time and stage, this is the main advantage of the AI-based data-driven techniques. The aeration efficiency can predict without performing the experiments, which ultimately saves time.

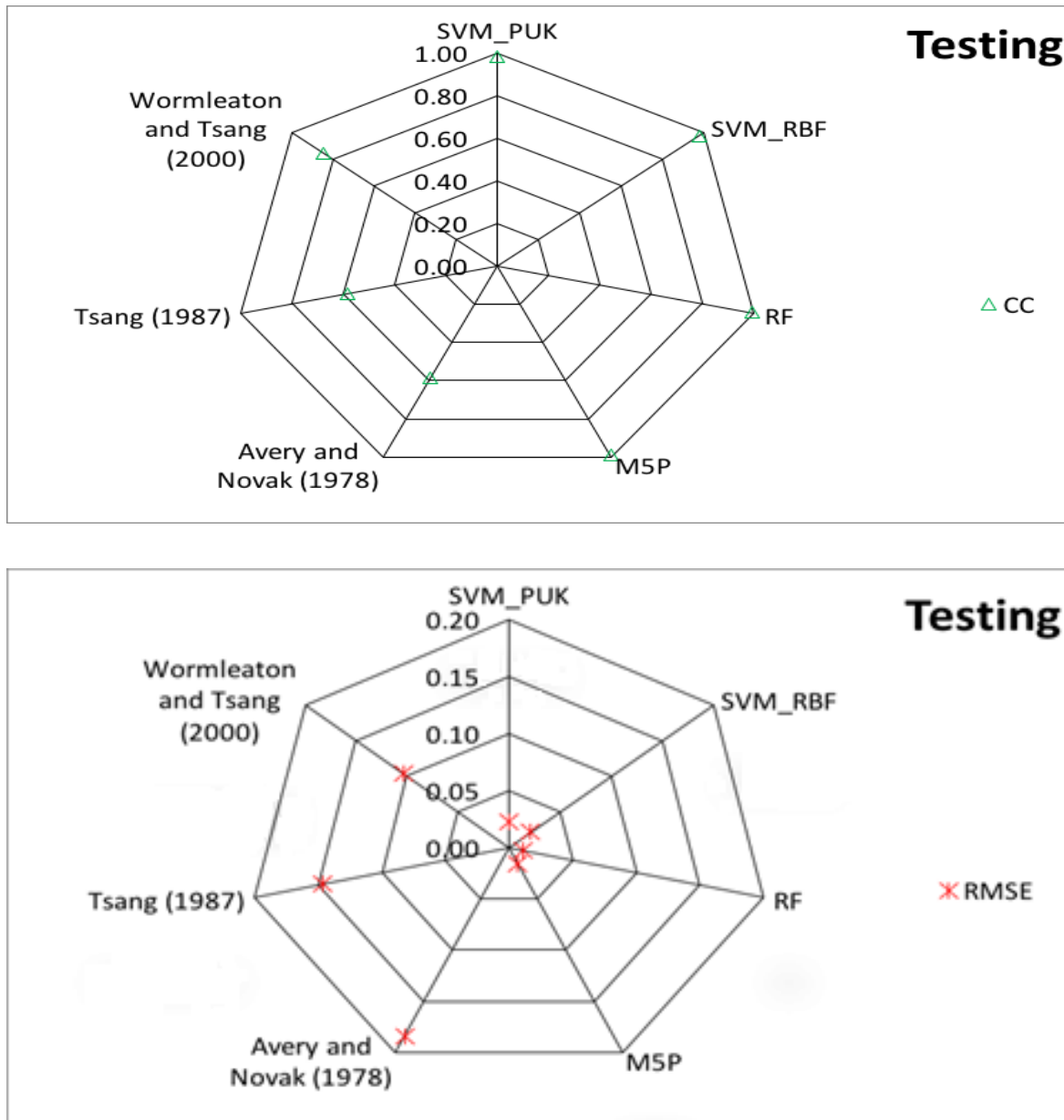


Fig. 9. The plot of values of CC and RMSE for different soft computing and conventional methods using the testing data set.

4.1. Sensitivity study

A sensitivity study was performed to find the mainly significant input parameter in estimating the Aeration efficiency (E_{20}) at LWs. The most effective parameters for estimation of Aeration efficiency (E_{20}) are determined by the RF method. At first, all the parameters regard to the table except E_{20} were considered as inputs for RF and then a single input parameter was eliminated and the model was reconstructed with the same configuration. The outcome of sensitivity analysis of RF is shown in Table 5. As seen in Table 4, the ratio of drop height and width of the channel is the most effective parameter in the estimation of Aeration efficiency (E_{20}) at LW.

Table 5

Performance of parameters for sensitivity analysis.

| Input Parameters | Removed Parameters | Target Parameter | RF | |
|------------------------------|--------------------|------------------|---------|--------|
| | | | Testing | |
| | | | CC | RMSE |
| Fr, Re, N, H/W, L/W, D/W, SF | | E_{20} | 0.9948 | 0.0112 |
| Re, N, H/W, L/W, D/W, SF | Fr | E_{20} | 0.9940 | 0.0121 |
| Fr, N, H/W, L/W, D/W, SF | Re | E_{20} | 0.9947 | 0.0114 |
| Fr, Re, H/W, L/W, D/W, SF | N | E_{20} | 0.9948 | 0.0113 |
| Fr, Re, N, L/W, D/W, SF | H/W | E_{20} | 0.9960 | 0.010 |
| Fr, Re, N, H/W, D/W, SF | L/W | E_{20} | 0.9951 | 0.011 |
| Fr, Re, N, H/W, L/W, SF | D/W | E_{20} | 0.9632 | 0.0334 |
| Fr, Re, N, H/W, L/W, D/W | SF | E_{20} | 0.9728 | 0.0256 |

5. Conclusions

This study is focused on the experimentation investigation and modeling of the aeration efficiency of the Labyrinth weir. The conclusion drawn from the experimental investigation is that oxygen transfer efficiency (E_{20}) increases with the number of the key as well as drop height. Also, it is found to be highest for rectangular plan-form labyrinth weir in comparison to other considered plan-form labyrinth weirs however E_{20} decreases with the increase of discharge for this dataset. Modeling results suggest that RF (random forest) technique is superior as it outperformed all the applied models however other AI-based models are also performing well and can be used in the estimation of E_{20} but classical models are incredibly giving poor results except Wormleaton and Tsang [13]. Furthermore, the sensitivity analysis suggests that that drop height at labyrinth weirs was the most significant variable for the estimation of E_{20} .

Authors contribution statement

Balraj Singh: Conceptualization, Balraj Singh; Parveen Sihag: Data curation; Aradhana; Investigation; Aradhana, Parveen Sihag: Methodology; Parveen Sihag: Software; Aradhana, Balraj Singh, Parveen Sihag: editing, review and Writing.

References

- [1] Gentilini B. Stramazzi con cresta a pianta obliqua ea zig-zag. Società Editrice Riviste Industrie Elettriche; 1941.
- [2] Taylor G. The performance of labyrinth weirs 1968.
- [3] Hay N, Taylor G. Performance and Design of Labyrinth Weirs. J Hydraul Div 1970;96:2337–57. doi:10.1061/JYCEAJ.0002766.

- [4] Crookston BM, Tullis BP. Discharge Efficiency of Reservoir-Application-Specific Labyrinth Weirs. *J Irrig Drain Eng* 2012;138:564–8. doi:10.1061/(ASCE)IR.1943-4774.0000451.
- [5] Christensen NA. Flow characteristics of arced labyrinth weirs. Utah State University; 2012.
- [6] Gameson ALH. Weirs and aeration of rivers. *J. Inst. Water Eng.*, 11. 1957.
- [7] Van der Kroon GTN, Schram AH. Weir aeration-part I: Single free fall. *H2O* 1969;22:528–37.
- [8] Nakasone H. Study of Aeration at Weirs and Cascades. *J Environ Eng* 1987;113:64–81. doi:10.1061/(ASCE)0733-9372(1987)113:1(64).
- [9] Avery ST, Novak P. Oxygen Transfer at Hydraulic Structures. *J Hydraul Div* 1978;104:1521–40. doi:10.1061/JYCEAJ.0005100.
- [10] Gulliver JS, Rindels AJ. Measurement of Air-Water Oxygen Transfer at Hydraulic Structures. *J Hydraul Eng* 1993;119:327–49. doi:10.1061/(ASCE)0733-9429(1993)119:3(327).
- [11] Wilhelms SC, Gulliver JS, Parkhill K. Reaeration at low-head hydraulic structures. ARMY ENGINEER WATERWAYS EXPERIMENT STATION VICKSBURG MS HYDRAULICS LAB; 1993.
- [12] Wormleaton PR, Soufiani E. Aeration Performance of Triangular Planform Labyrinth Weirs. *J Environ Eng* 1998;124:709–19. doi:10.1061/(ASCE)0733-9372(1998)124:8(709).
- [13] Wormleaton PR, Tsang CC. Aeration Performance of Rectangular Planform Labyrinth Weirs. *J Environ Eng* 2000;126:456–65. doi:10.1061/(ASCE)0733-9372(2000)126:5(456).
- [14] Singh B. Prediction of the sodium absorption ratio using data-driven models: a case study in Iran. *Geol Ecol Landscapes* 2020;4:1–10. doi:10.1080/24749508.2019.1568129.
- [15] Baylar A, Bagatur T. Study of aeration efficiency at weirs. *Turkish J Eng Environ Sci* 2000;24:255–64.
- [16] Baylar A, Hanbay D, Batan M. Application of least square support vector machines in the prediction of aeration performance of plunging overfall jets from weirs. *Expert Syst Appl* 2009;36:8368–74. doi:10.1016/j.eswa.2008.10.061.
- [17] Vand AS, Sihag P, Singh B, Zand M. Comparative Evaluation of Infiltration Models. *KSCE J Civ Eng* 2018;22:4173–84. doi:10.1007/s12205-018-1347-1.
- [18] Kumar M, Ranjan S, Tiwari NK. Oxygen transfer study and modeling of plunging hollow jets. *Appl Water Sci* 2018;8:1–15.
- [19] Kumar M, Ranjan S, Tiwari NK, Gupta R. Plunging hollow jet aerators - oxygen transfer and modelling. *ISH J Hydraul Eng* 2018;24:61–7. doi:10.1080/09715010.2017.1348264.
- [20] Bilhan O, Emin Emiroglu M, Kisi O. Application of two different neural network techniques to lateral outflow over rectangular side weirs located on a straight channel. *Adv Eng Softw* 2010;41:831–7. doi:10.1016/j.advengsoft.2010.03.001.
- [21] Emiroglu ME, Bilhan O, Kisi O. Neural networks for estimation of discharge capacity of triangular labyrinth side-weir located on a straight channel. *Expert Syst Appl* 2011;38:867–74. doi:10.1016/j.eswa.2010.07.058.
- [22] Kisi O, Emin Emiroglu M, Bilhan O, Guven A. Prediction of lateral outflow over triangular labyrinth side weirs under subcritical conditions using soft computing approaches. *Expert Syst Appl* 2012;39:3454–60. doi:10.1016/j.eswa.2011.09.035.
- [23] Zhang W, Li H, Li Y, Liu H, Chen Y, Ding X. Application of deep learning algorithms in geotechnical engineering: a short critical review. *Artif Intell Rev* 2021. doi:10.1007/s10462-021-09967-1.
- [24] Pal M, Singh NK, Tiwari NK. Pier scour modelling using random forest regression. *ISH J Hydraul Eng* 2013;19:69–75. doi:10.1080/09715010.2013.772763.

- [25] Zhang W, Zhang R, Wu C, Goh ATC, Lacasse S, Liu Z, et al. State-of-the-art review of soft computing applications in underground excavations. *Geosci Front* 2020;11:1095–106. doi:10.1016/j.gsf.2019.12.003.
- [26] Pandhiani SM, Sihag P, Shabri A Bin, Singh B, Pham QB. Time-Series Prediction of Streamflows of Malaysian Rivers Using Data-Driven Techniques. *J Irrig Drain Eng* 2020;146:04020013. doi:10.1061/(ASCE)IR.1943-4774.0001463.
- [27] Roushangar K, Alami MT, Majedi Asl M, Shiri J. Modeling discharge coefficient of normal and inverted orientation labyrinth weirs using machine learning techniques. *ISH J Hydraul Eng* 2017;23:331–40. doi:10.1080/09715010.2017.1327333.
- [28] Ohtsu I, Yasuda Y, Takahashi M. Discussion of onset of skimming flow on stepped spillways. *J Hydraul Eng ASCE* 2001;127:522–4.
- [29] Tsang C. Hydraulic and aeration performance of labyrinth weirs. 1987.
- [30] Gulliver JS, Thene JR, Rindels AJ. Indexing Gas Transfer in Self-Aerated Flows. *J Environ Eng* 1990;116:503–23. doi:10.1061/(ASCE)0733-9372(1990)116:3(503).
- [31] Tebbutt THY. Reaeration performance of stepped cascades. *J. Inst. of Water Engrs. and Sci.*, 31, 285-297. 1977.
- [32] Cortes C, Vapnik V. Support-vector networks. *Mach Learn* 1995;20:273–97. doi:10.1007/BF00994018.
- [33] Vapnik V. *Statistical Learning Theory*, New York 1998.
- [34] Quinlan JR. Learning with continuous classes. 5th Aust. Jt. Conf. Artif. Intell., *WORLD SCIENTIFIC*; 1992, p. 343–8. doi:10.1142/9789814536271.
- [35] Breiman L. Random forests—random features 1999.
- [36] Karami H, Ghazvinian H, Dehghanipour M, Ferdosian M. Investigating the Performance of Neural Network Based Group Method of Data Handling to Pan’s Daily Evaporation Estimation (Case Study: Garmsar City). *J Soft Comput Civ Eng* 2021;5:1–18.